

















# Application-specific integrated circuits for X-ray imaging and neurobiology

Piotr Kaczmarczyk , Łukasz Kadłubowski , Krzysztof Kasiński ,  
Rafał Kłeczek , Piotr Kmon , Anna Koziół ,  
Aleksandra Krzyżanowska , Piotr Maj , Piotr Otfinowski ,  
Marek Miśkiewicz , Paweł Skrzypiec , Robert Szczygieł ,  
Grzegorz Węgrzyn , Weronika Zubrzycka , Mirosław Żołądz ,  
Paweł Gryboś 

AGH University of Science and Technology, Faculty of Electrical Engineering, Automatics, Computer Science and Biomedical Engineering, Krakow, Poland

---

**Abstract:** The dynamic development of multiple types of sensors of physical quantities requires the development of new electronic systems adapted to them. High-density multichannel ionizing radiation sensors are used in industrial and medical imaging as well as in high-energy physics experiments. Likewise, multichannel sensor systems are used to record biomedical signals. In both cases, when reading sensors, specialized ASIC integrated circuits are used, which allow the construction of detection systems with good measurement parameters while maintaining low power consumption. The following article presents selected examples of integrated readout circuits designed in the microelectronic group of the Department of Measurement and Electronics at AGH UST in Krakow.

**Keywords:** integrated circuits, sensor matrices, ionizing radiation imaging, recording of neurobiological signals

## SPECJALIZOWANE UKŁADY SCALONE NA POTRZEBY OBRAZOWANIA PROMIENIOWANIA X

**Streszczenie:** Dynamiczny rozwój wielorakiego rodzaju sensorów wielkości fizycznych wymaga opracowywania coraz nowszych systemów elektronicznych do nich dostosowanych. Wielokanałowe sensory promieniowania jonizującego o dużej gęstości upakowania znajdują zastosowanie w obrazowaniu przemysłowym i medycznym oraz eksperymentach fizyki wysokich energii. Podobnie wielokanałowe systemy sensorów są używane do rejestracji sygnałów biomedycznych. W obu przypadkach przy odczycie sensorów niezastąpioną rolę odgrywają specjalizowane układy scalone ASIC, które pozwalają na budowanie systemów detekcyjnych o dobrych parametrach pomiarowych przy zachowaniu niskiego poboru mocy. Artykuł prezentuje wybrane przykłady skalonych układów odczytowych zaprojektowanych w grupie mikroelektronicznej Katedry Me-trologii i Elektroniki AGH w Krakowie.

**Słowa kluczowe:** układy scalone, matryce sensorów, obrazowanie promieniowania jonizującego, rejestracja sygnałów neurobiologicznych

## 1. Introduction

Experimental techniques in physics, material science, biology, and medicine want to profit from the advantages of VLSI technology by using a new generation of electronic measurement systems based on parallel signal processing from multi-element sensors. In most cases, key problems for building such a system are multichannel mixed-mode application specific integrated circuits (ASIC), which are capable to process small-amplitude signals from a multi-element sensor. This paper presents examples of ASICs that were designed and tested in the Department of Measurement and Electronics, AGH University of Science and Technology, Kraków. These ASICs, given the original solutions implemented and due to their universal properties, are used in different applications (X-ray imaging, neurobiology, etc.) and are significant milestones in experimental techniques.

## 2. ASICs for hybrid pixel detectors

Hybrid Pixel Detectors (HPDs) are becoming more and more important in many different industrial and scientific fields (Rossi et al. 2006). HPD usually consists of a pixelated sensor and readout front-end electronics of the pixel architecture connected by the bump-bonding technique (see Fig. 1a). HPD allows for the use of different sensor materials depending on X-ray energies used in applications, while readout IC can be the same. Depending on the application requirements, the readout IC can be designed and fabricated using the advanced technology offered by the microelectronic industry.

The general idea of HPD operation is as follows. When an X-ray photon hits the detector, it is converted into a short current pulse carrying a charge proportional to the photon energy (e.g. an 8 keV X-ray photon generates a charge of 2200  $e^-$  in a silicon detector). This current pulse flows into the readout front-end electronics input and is processed according to the required functionality. Taking into account the input signals processing scheme applied in readout front-end electronics, HPD can be divided into two main groups: detectors based on input charges integration (summation) and working in the Single Photon Counting (SPC) mode. In charge integration-type detectors, the input charges (generated by consecutive impinging photons) are summed up in each pixel during a given exposure time. In SPC type detectors, each impinging photon is processed independently in each channel of the readout front-end electronics channel in photon-by-photon order (Rossi et al. 2006, Ballabriga et al. 2006, Dinapoli et al. 2013, Maj et al. 2013, Grybos et al. 2016, Zhang et al. 2017, Nakaye et al. 2021)

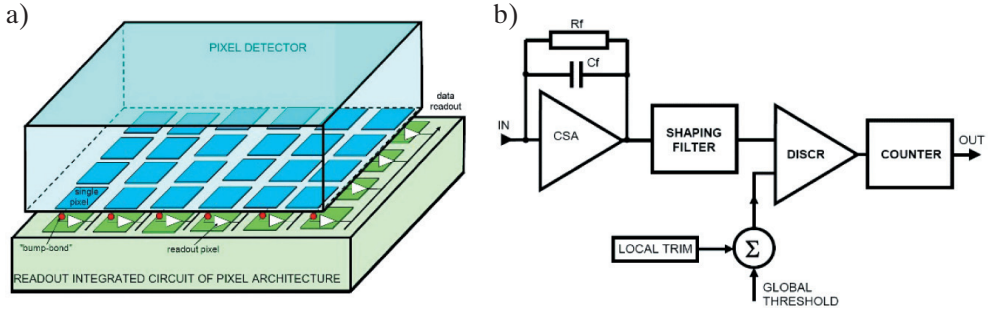


**Fig. 1.** Hybrid pixel detector: sensor and readout chip are connected using the bump-bonding technique (a); simplified architecture of a single readout channel operating in a single-photon counting mode (b)

The single readout front-end channel usually consists of a Charge Sensitive Amplifier (CSA), a pulse shaping amplifier (shaper), a discriminator, and a counter (see Fig. 1b). The input pulse current flows into the CSA input generating a voltage step at its output, which is then amplified and filtered by the shaper stage. Depending on the shaper output pulse amplitude, the pixel counter value is incremented by one if this amplitude is higher than a set threshold (see Fig. 2). The main advantages of the SPC detectors over the integrating type detectors are very high dynamic range, noiseless imaging (by properly setting the discriminator threshold only valid counts coming from photons are registered), and the possibility of counting photons within a given energy window (in systems where two or more discriminators and thresholds are used).

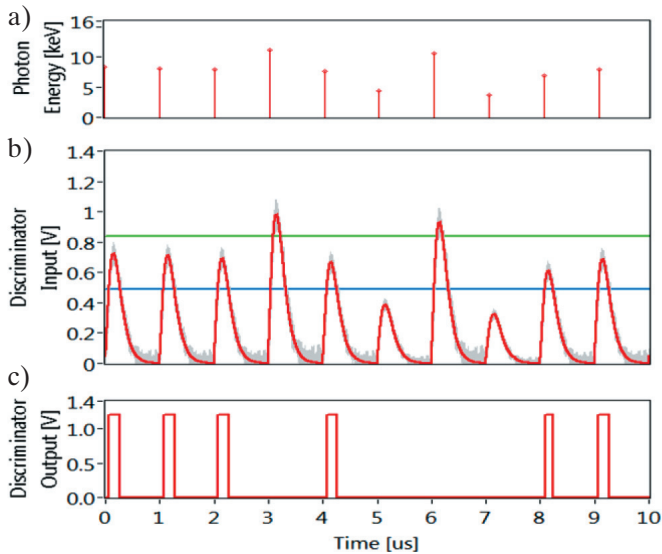


**Fig. 2.** Pulse processing in a single-photon counting system:  
a) photons of different energies hit in a given pixel; b) shaper output voltage pulses;  
c) discriminator output pulses corresponding to the set threshold

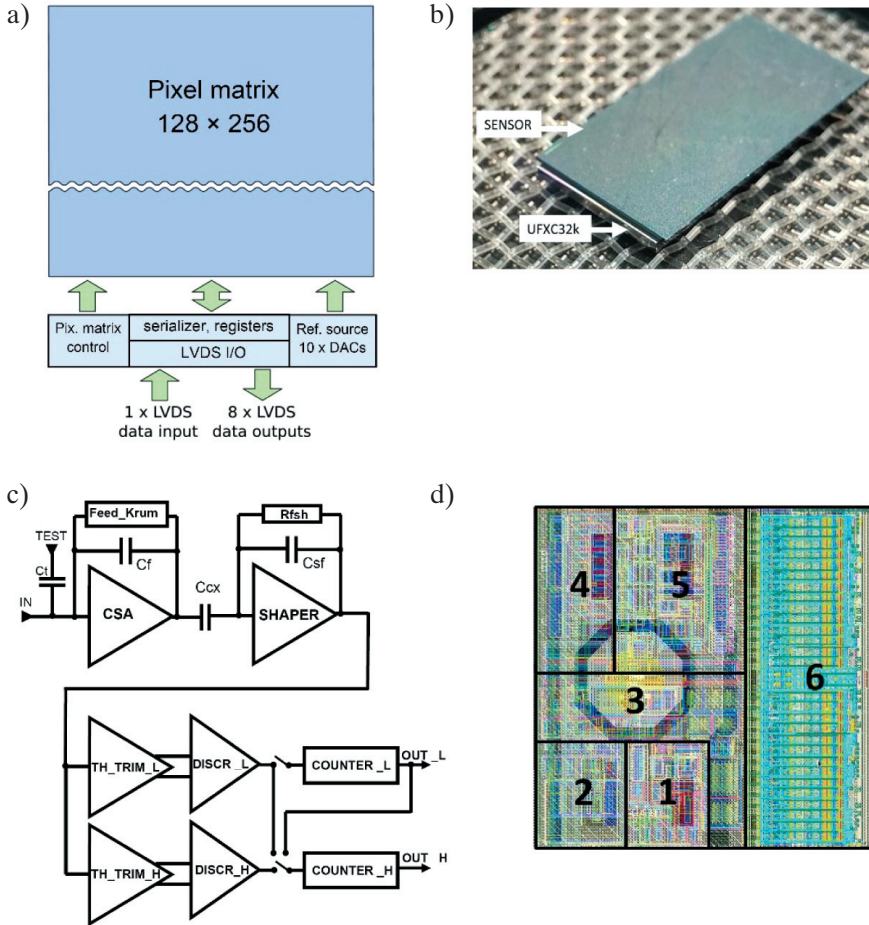


**Fig. 3.** UFCX32k IC: a) simplified block diagram of the readout IC; b) IC photo; c) simplified block diagram of a single pixel; d) layout of a single pixel with marked functional blocks: 1 – CSA core amplifier, 2 – Krummenacher structure, 3 – shaper, 4 – in-pixel biasing circuit, 5 – TH\_SET, TRIM\_DAC, DISCR, 6 – counters and registers

For practical applications, large-area ICs with thousands of channels play a crucial role, especially if they allow the building of large-area HPDs. An example of such a solution was developed recently at the AGH UST IC called UFCX32k (Ultra Fast X-ray Chip with 32k channels) (see Fig. 3) (Grybos et al. 2013). The UFCX32k IC, manufactured using CMOS 130 nm technology, has dimensions of 9.64 mm × 20.15 mm and contains approximately 50 million transistors. The core of the IC is a matrix of 128 × 256 square pixels with 75 μm pixel pitch. Each pixel operates in SPC mode with two thresholds that work independently. A single pixel contains a CSA with a Krummenacher feed-back discharge circuit (Feed\_Krum), a shaper with a peaking time of 40 ns, threshold-

-setting blocks (TH\_SET), and two discriminators (DISCR) and two 14-bit ripple counters (COUNTER). Each discriminator is equipped with a trimming DAC (TRIM\_DAC) used for dc offset correction. The analog front-end electronics allow for the processing of sensor signals of both polarities (holes or electrons), which allows for testing with different detector materials (Si, GaAs, CdTe, etc.). During the IC data readout phase, the counters in each column form a shift register. The data from the shift registers are loaded bit by bit into the peripheral fast 128-bit register and shifted out of the UFX32k IC via 8 LVDS parallel lines.

The measured equivalent noise charge for the standard settings is equal to  $123\text{ e}^-$  rms (for a peaking time of 40 ns), and each pixel dissipates  $26\text{ }\mu\text{W}$ . Thanks to the use of trimming DACs working in each pixel independently, an effective offset spread calculated to the input is only  $9\text{ e}^-$  rms with a gain spread of 2%. The readout front-end electronics deadtime can be set as low as 85 ns. As a result of the IC analog part of the IC and good noise performance, a satisfying image, like the one presented in Figure 4, can be achieved without any software correction.

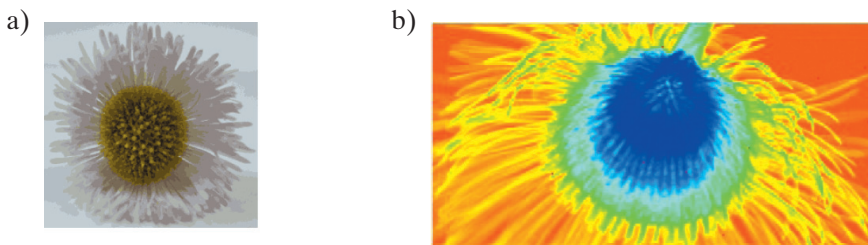


**Fig. 4.** A daisy: a) photo; b) the first radiogram taken with the UFX32k bump-bonded to Si pixel detector

An experimental measurement system based on the UFX32k IC allows the detector to perform novel experiments at a synchrotron radiation source. Due to the very high frame rate, coping with a high intensity flux of X-ray photons, and the possibility of zero-dead-time readout mode, the prepared detector is a good candidate for time-resolved research studies. A dedicated system was built and used at the US APS at Argonne National Laboratory. The application was high-speed and small-angle X-ray correlation spectroscopy.

Thanks to the described system it was possible to examine the formation and dissolution of gels composed of intermediate volume-fraction nanoparticles with temperature-dependent short-range attractions using small-angle X-ray scattering, photon correlation spectroscopy, and rheology to obtain nanoscale and macroscale sensitivity to structure and dynamics (Zhang et al. 2017). A similar system based on the UFX32k IC was built for Synchrotron Soleil in France, where it was also used for high-speed time-resolved experiments with synchrotron radiation (Nakaye et al. 2021).

### 3. STS-XYTER IC for CBM experiment

Particle tracking in the physics experiment is an important research topic for many researchers and IC designers worldwide. Facilities with a large research infrastructure are funded by governments of many countries to study various areas of modern physics. This research can only be performed with specific measurement equipment. ASICs are needed to obtain the best achievable radiation imaging, given the area and power limitations.

The Compressed Baryonic Matter (CBM) experiment (Heuser 2013) is one of the pillars of the new research facility established in Darmstadt, Germany, in the vicinity of the renowned GSI (Helmholtzzentrum Fuer Schwerionenforschung) called FAIR (Facility for Antiproton and Ion Research), where more than 55 institutions from 15 countries contribute to building it.

The authors carried out research targeting radiation imaging techniques in two detector layers of the CBM experiment, i.e. tracking detectors called STS (Silicon Tracking System) and MuCH (Muon Chamber). Both systems required a low-noise, self-triggered, multichannel IC capable of measuring both arrival time and amplitude of the short charge pulses.

In the first stage, the research identified the optimum charge pulse amplification and digitization technique. Several techniques were investigated:

- Time-over-Threshold method, offering low-power analog-to-digital conversion by Wilkinson-type processing (Kasinski et al. 2011).
- CSA with two paths supplied with different shapers in each channel independently. One of them (fast shaper) was optimized for time measurement and was followed by a leading-edge discriminator and a timestamp counter. Another (slow shaper) was optimized for amplitude measurement and was followed by a continuous-time FLASH analog-to-digital converter with a digital peak detector. Extensive studies of noise contributions and the selection of optimal shaping amplifiers were carried out (Kasinski et al. 2014).

It became clear that the power budget and noise requirements allowed one to use the latter solution, with the channel architecture shown in Figure 5. Enhanced by multiple features allowing flexibility across different operating conditions (e. g. configurable shaping time, CSA gain, trimming options of the discriminator offsets and gain, optimized ESD protection structure, CSA reset capability) has been verified during testing of the prototypes (Kasinski et al. 2018) (see Figs. 6–8), and the tests of ‘Mini-STS’, which is a demonstrator of the entire detector chain. This has shown that the architecture developed is ready for volume production.



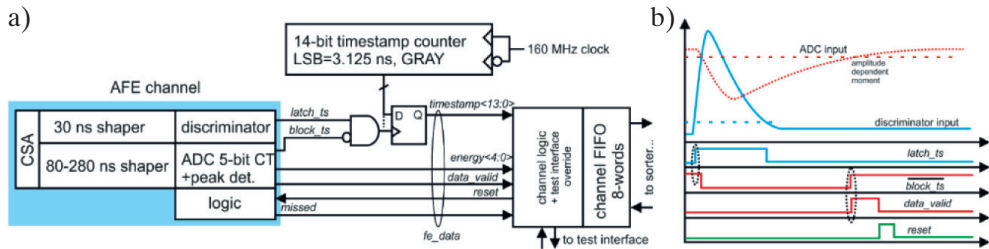


**Fig. 5.** The architecture of a single channel of the STS-XYTER chip (a); exemplary waveforms (b)

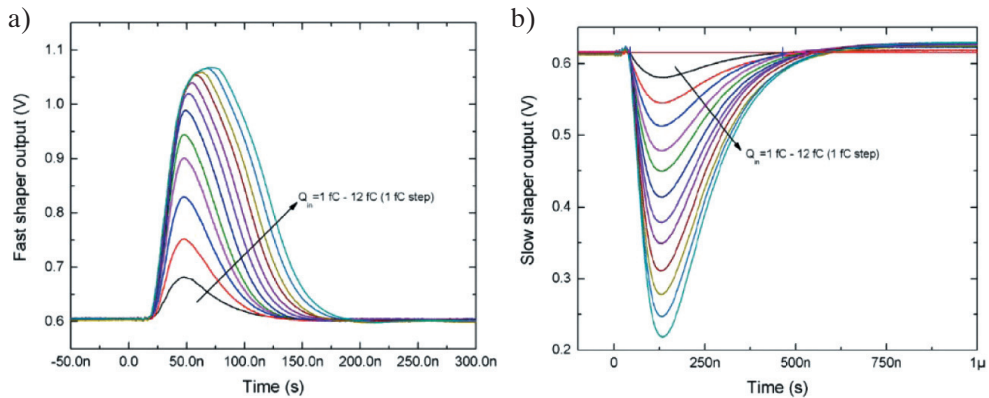


**Fig. 6.** Exemplary waveforms measured at the output of the fast shaper of the prototype chip for the input charge  $Q_{in} = 1\text{--}12$  fC (hole collection). The fast shaper peaking time is equal to 30 ns, and the CSA gain is set to a nominal value for STS. No sensor is attached (a). Exemplary waveforms at the slow shaper output for the input charge  $Q_{in} = 1\text{--}12$  fC (b)

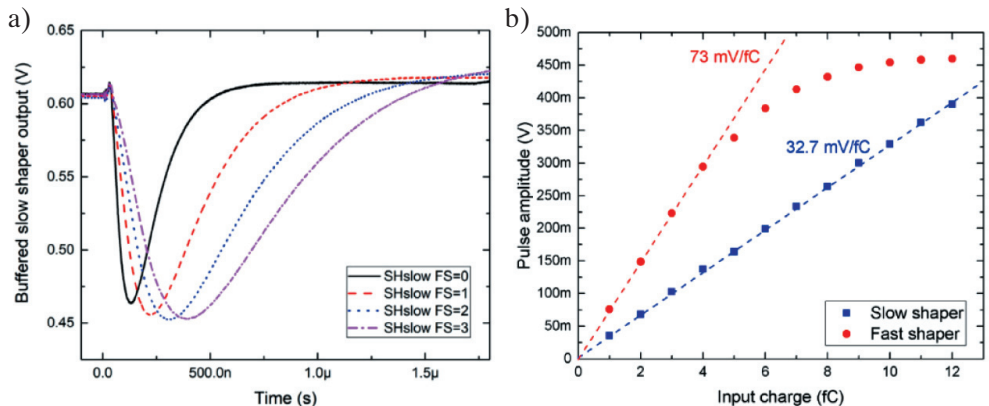


**Fig. 7.** Exemplary slow shaper waveforms for different settings of shaping time. The typical input charge  $Q_{\text{in}} = 4$  fC (holes collection) is applied. No sensor is attached (a). Gain characteristics of the fast and slow shapers for a nominal STS detector gain setting, measured in the test channels with buffered analog outputs (b)

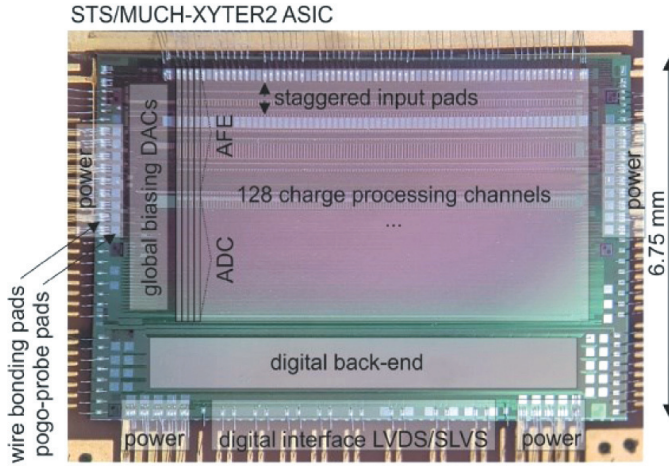


**Fig. 8.** Photo of the STS-XYTER ASIC with the main building blocks marked

The STS-XYTER family (Kasinski and Zubrzycka 2020) evolved during a series of three full-size chip prototypes, with a similar layout (see Fig. 8). Each of them is a 128-channel amplitude and time digitization solution with a digital back-end and a fast digital interface. The latest version, SMX2.2 (Schmidt et al. 2020), was approved for series production and will be used to assemble detector readout systems consisting of tens of thousands of these ASICs.

#### 4. ASIC for neurobiology applications

Existing technologies allow building systems made up of sensors combined with electronics. Whenever such systems need to be very small, have rich functionality, low power consumption, batteryless supply, and architecture allowing multisite signal processing (see Fig. 9), modern technologies are the only way to satisfy these requirements. These may be micro-electron-mechanical systems (MEMS) and very-large-scale integration (VLSI) technologies for sensors and electronics production, respectively. Many different biomedical experiments involve the use of advanced electronics to record biomedical signals (Narayan 2018, Saltzman 2015, Fischer et al. 2015, Shin et al. 2021). These are mainly run to extract valuable information regarding the human nervous system or to support people in their daily lives. The common attribute of the above-mentioned applications is the fact that they need to be very small; otherwise, these could not allow for increasing spatial resolution of the recordings, and could they be implanted into the body for experiment purposes.



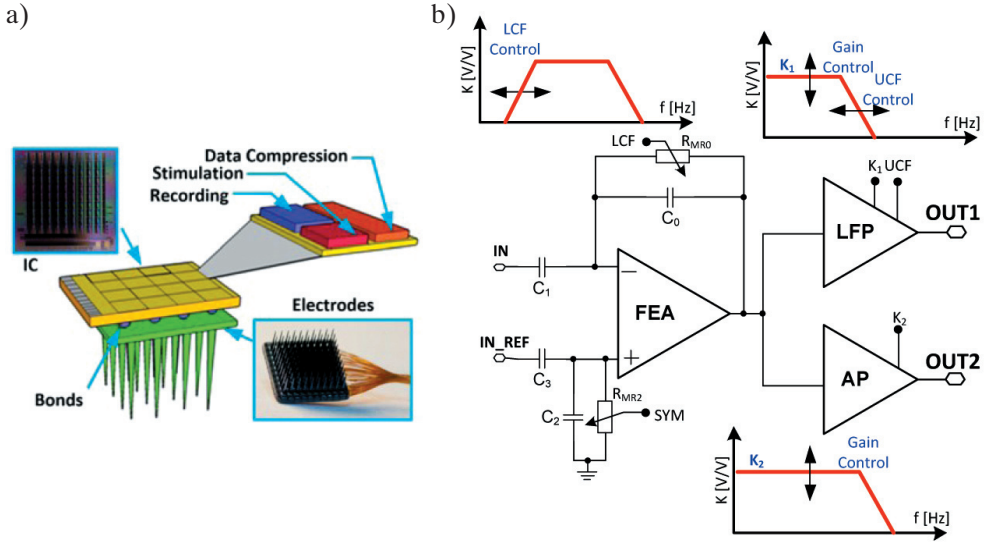


**Fig. 9.** Conceptual view of the implantable multichannel integrated system for biomedical experiments (a); block idea of the proposed recording channel (b)

#### 4.1. Recording channel architecture

The main task of the recording channels is to perform amplification and filtration of weak biomedical signals that are transmitted to the amplifiers' input by the recording electrodes. Here, recording electrodes are used as an ionic to electrons transducer and, more importantly, are potentially a source of large DC voltage offsets that need to be separated from the amplifier input not to lead to its saturation and to avoid any current flow at the electrode-electronics interface. Having looked at the different species of biomedical signals (see Tab. 1), it can be seen that the front-end amplifier should have low input-referred noise and the ability to change both its frequency bandwidth and voltage gain. Furthermore, the analog recording part should provide conditioned biomedical signals to the consecutive blocks in a way (like analog to digital converters) that efficiently uses their conversion range or speed. Therefore, we decided to compose the analog recording part with a few blocks as shown in Figure 9b.

The preamplifier is based on an operational amplifier that works with capacitive feedback (Harrison 2008, Rodríguez-Pérez et al. 2014). Due to its architecture, a proposed amplifier has an inherent AC coupling at the input. The voltage gain of this stage is established by the ratio of  $C_0/C_1$ , while the lower cut-off frequency is proportional to  $1/(2\pi R_{MR0}C_1)$ . To obtain lower cut-off frequencies much below 1 Hz (see Tab. 1), the  $R_{MR0}C_1$  time constant should be very high. Therefore,  $R_{MR0}$  is based on a PMOS transistor that works in a subthreshold region (its channel dimensions

are  $W/L = 0.4 \mu\text{m}/50 \mu\text{m}$ ) while  $C_1$  is built on a MIM capacitor (metal insulator metal). The upper cut-off frequency is proportional to the ratio ( $G_m$  is the transconductance of the amplifier, while  $C_L$  is the loading capacitance). To record different biomedical signals and compensate for circuitry mismatches, we decided to independently control the lower and upper cut-off frequency and voltage gain in each recording channel. This is realized by in-channel digital-to-analog converters in channel or transistor-based switches.

**Table 1**  
Typical biomedical signal parameters

Biomedical signals	Amplitudes	Frequency band [Hz]
Local Field Potential (LFP)	$10 \mu\text{V} - 5 \text{ mV}$	$10 - 500$
Action Potentials (AP)	$10 \mu\text{V} - 500 \mu\text{V}$	$300 - 7000$
EEG	$1 \mu\text{V} - 10 \mu\text{V}$	$<1 - 100$
ECG	$1 \text{ mV} - 10 \text{ mV}$	$5 - 500$
EMG	$100 \mu\text{V} - 10 \text{ mV}$	$20 - 1000$

Also, it can be seen that, whenever there is a need to record neurobiological signals with one circuitry, it is required to set different front-end parameters. Therefore, a conventional single-path recording channel is not an efficient solution. If, for example, LFP and AP signals are considered to be recorded simultaneously (see Tab. 1), one needs to set the proper sampling frequency to avoid aliasing, and this results in an unnecessarily high sampling frequency for LFP signals. Additionally, as the LFP signals are a few times higher in their amplitudes compared to the AP signals, one needs to set the correct voltage gain setting not to exceed the amplifier's linear region. As a consequence, the voltage gain may be too small for AP signals, resulting in a higher ADC resolution requirement to properly reconstruct small AP signals. Having all of these in mind, the particular recording channel was divided into two individual conditioning paths, that is, one for slow signal processing and the other for fast signal processing, as shown in Figure 9b.

## 4.2. Multichannel recording system

On the basis of the designed ICs, we developed different versions of multichannel systems for biomedical experiments. An example is shown in Figure 10 which is constructed of 16 channel electrodes and was successfully used for in vivo and in vitro experiments carried out in cooperation with neurobiologists from Jagiellonian University and Lodz University (Zoladz et al. 2014) (see Fig. 11).

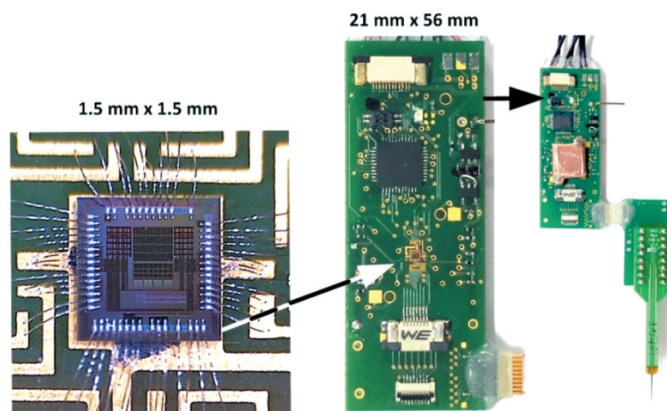


**Fig. 10.** Miniaturized conditioning module equipped with Integrated Circuit and 16 channel NeuroNexus provided electrodes

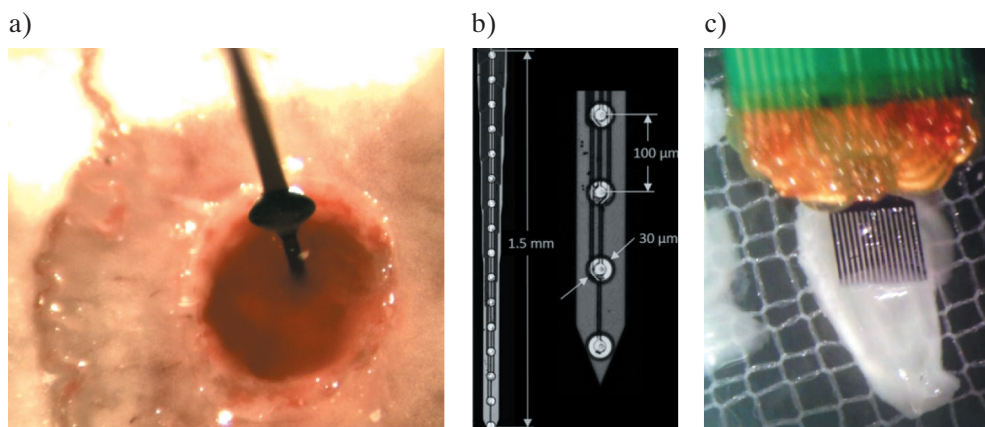


**Fig. 11.** Photos of neurobiological experiments: a) in vivo experiment showing the electrode inserted into the brain of rats; b) detailed view of the electrodes used in the presented experiment; c) in vitro experiment where fork-shaped electrodes are used to record signals from the hippocampus

The designed ICs were also used in the neurobiological experiments performed in collaboration with Qwane Biosciences SA, Lausanne, Switzerland. The idea of this experiment was to perform a first feasibility study of the propagation speed of the measure of neuronal signals along isolated axons (see Fig. 12). The motivation of this experiment was to find a way that allows the study of the propagation characteristics of neuronal signals along the axons, as impairment of axonal propagation is often a consequence of neurodegenerative diseases. This approach could lead to a platform for drug screening applications in which neuronal protection or recovery could be monitored by the speed of propagation along the axons. Therefore, to perform this experiment, the 256 channel in vitro recording platform (Zoladz 2013) was adapted to a specially

developed Micro-Electrode Array (MEA) device. Exemplary recording results may be seen in Figure 13.

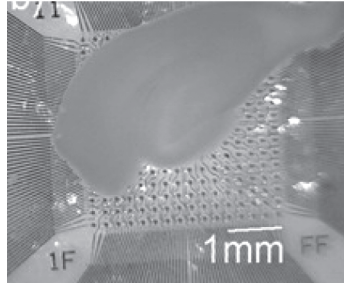


**Fig. 12.** Detailed photos of the multichannel electrodes used for in vitro experiments with the hippocampus laid over the recording electrodes

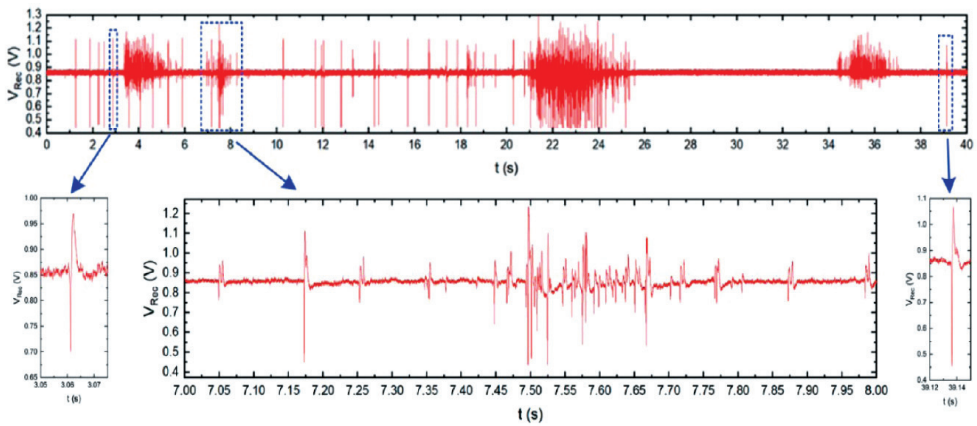


**Fig. 13.** Typical neurobiological signals were recorded by the designed chip. The magnified bottom-placed picture shows several signals that differ in amplitudes and shapes from different axons

## 5. Summary

The following article shows selected examples of integrated readout circuits designed in the Department of Measurement and Electronics at AGH UST in Krakow. These ICs are used worldwide in different measurements during X-ray imaging, particle physics, and neurobiology experiments and are significant milestones in these experimental techniques.

### Acknowledgment

The authors thank EUROPRACTICE for professional service, the Cadence Academic Network for helpful discussion, and the National Science Center, Poland.

Expression of gratitude goes to our colleagues and collaborators from Argonne National Laboratory, Synchrotron Soleil, CBM Collaboration, and Rigaku Corporation.

## References

- Ballabriga R., Alozy J., Blaj G., Campbell M., Fiederle M., Frojdh E., Heijne E.H.M. et al., 2013, *The Medipix3RX: a high resolution, zero dead-time pixel detector readout chip allowing spectroscopic imaging*, Journal of Instrumentation, vol. 8, no. 02, C02016. <https://doi.org/10.1088/1748-0221/8/02/c02016>.
- Dinapoli R., Bergamaschi A., Greiffenberg D., Henrich B., Horisberger R., Johnson I., Mozzanica A. et al., 2013, *EIGER characterization results*, Nuclear Instruments and Methods in Physics Research Section A: Accelerators, Spectrometers, Detectors and Associated Equipment, vol. 731, pp. 68–73. <https://doi.org/10.1016/j.nima.2013.04.047>.
- Fischer A.C., Forsberg F., Lapisa M., Bleiker S.J., Stemme G., Roxhed N., Niklaus F., 2015, *Integrating MEMS and ICs*, Microsystems and Nanoengineering, vol. 1, no. 1, 15005. <https://doi.org/10.1038/micronano.2015.5>.
- Grybos P., Kmon P., Maj P., Szczygiel R., 2016, *32k Channel Readout IC for Single Photon Counting Pixel Detectors with 75  $\mu\text{m}$  Pitch, Dead Time of 85 ns, 9  $e^-$  rms Offset Spread and 2% rms Gain Spread*, IEEE Transaction on Nuclear Science, vol. 63, no. 2, pp. 1155–1161. <https://doi.org/10.1109/TNS.2016.2523260>.
- Harrison R.R., 2008, *The Design of Integrated Circuits to Observe Brain Activity*, Proceedings of IEEE, vol. 96, no. 7, pp. 1203–1216. <https://doi.org/10.1109/JPROC.2008.922581>.
- Heuser J., 2013, *The Compressed Baryonic Matter Experiment at FAIR*, Nuclear Physics A, vol. 1005, 121945. <https://doi.org/10.1016/j.nuclphysa.2020.121945>.
- Kasinski K., Zubrzycka W., 2020, *Overview of Microelectronic Circuits Designed at AGH University for the CBM Experiment*, Acta Physica Polonica. B, Proceedings Supplement, vol. 13, no. 4, pp. 885–891. <https://doi.org/10.5506/APhysPolBSupp.13.885>.
- Kasinski K., Szczygiel R., Grybos P., 2011, *TOT02, a time-over-threshold based readout chip in 180 nm CMOS process for long silicon strip detectors*, [in:] 2011 IEEE Nuclear science symposium and Medical imaging conference: 18<sup>th</sup> international workshop on Room-temperature semiconductor x-ray and gamma-ray detectors: industrial exhibition (short courses) special focus workshops: Valencia, Spain, 23–29 October 2011, IEEE, Piscataway, pp. 631–636. <https://doi.org/10.1109/NSSMIC.2011.6153981>.
- Kasinski K., Kleczek R., Otfinowski P., Szczygiel R., Grybos P., 2014, *STS-XYTER, a high count-rate self-triggering silicon strip detector readout IC for high resolution time and energy measurements*, [in:] 2014 IEEE Nuclear Science Symposium and Medical Imaging Conference (NSS/MIC): 8–15 Nov. 2014, Seattle, USA, IEEE, Piscataway, pp. 1–6. <https://doi.org/10.1109/NSSMIC.2014.7431048>.

- Kasinski K., Rodriguez-Rodriguez A., Lehnert J., Zubrzycka W., Szczygiel R., Otfiowski P., Kłeczek R. et al., 2018, *Characterization of the STS/MUCH-XYTER2, a 128-channel time and amplitude measurement IC for gas and silicon microstrip sensors*, Nuclear Instruments & Methods in Physics Research. Section A, Accelerators, spectrometers, detectors and associated equipment, vol. 908, pp. 225–235. <https://doi.org/10.1016/j.nima.2018.08.076>.
- Maj P., Grybos P., Szczygiel R., Zoladz M., Sakumura T., Tsuji Y., 2013, *18k Channels single photon counting readout circuit for hybrid pixel detector*, Nuclear Instruments & Methods in Physics Research. Section A, Accelerators, spectrometers, detectors and associated equipment, vol. 697, pp. 32–39. <https://doi.org/10.1016/j.nima.2012.08.103>.
- Nakaye Y., Sakumura T., Sakuma Y., Mikusu S., Dawiec A., Orsini F., Grybos P. et al., 2021, *Characterization and performance evaluation of the XSPA-500k detector using synchrotron radiation*, Journal of Synchrotron Radiation, vol. 28, no. 2, pp. 439–447. <https://doi.org/10.1107/S1600577520016665>.
- Narayan R. (ed.), 2018, *Encyclopedia of Biomedical Engineering*, 1<sup>st</sup> ed. Elsevier.
- Rodríguez-Pérez A., Delgado-Restituto M., Darie A., Soto-Sánchez C., Fernández-Jover E., Rodríguez-Vázquez Á., 2014, *A 330μW, 64-channel neural recording sensor with embedded spike feature extraction and auto-calibration*, [in:] *2014 IEEE Asian Solid-State Circuits Conference*, IEEE, Piscataway, pp. 205–208. <https://doi.org/10.1109/ASSCC.2014.7008896>.
- Rossi L., Fischer P., Rohe T., Wermes N., 2006, *Pixel Detectors: From Fundamentals to Applications*, Particle Acceleration and Detection, Springer-Verlag Berlin Heidelberg.
- Saltzman W.M., 2015, *Biomedical Engineering: Bridging Medicine and Technology*, 2<sup>nd</sup> ed. Cambridge University Press, Cambridge.
- Schmidt C., Lehnert J., Kasiński K., 2020, *New and final ASIC STS-XYTER Version 2.2*, CBM Progress Report 2020.
- Shin H., Jeong S., Lee J.H., Sun W., Choi N., Cho I.J., 2021, *3D high-density microelectrode array with optical stimulation and drug delivery for investigating neural circuit dynamics*, Nature Communications, vol. 12, no. 1, 492. <https://doi.org/10.1038/s41467-020-20763-3>.
- Zhang Q., Bahadur D., Dufresne E., Grybos P., Kmon P., Leheny R., Maj P. et al., 2017, *Dynamic Scaling of Colloidal Gel Formation at Intermediate Concentrations*, Physical Review Letters, vol. 119, no. 17, 178006. <https://doi.org/10.1103/PhysRevLett.119.178006>.
- Zoladz M., 2013, *A System for 256-Channel in Vitro Recording of the Electrophysiological Activity of Brain Tissue*, Metrology and Measurement. Systems, vol. 20, no. 3, pp. 371–384. <https://doi.org/10.2478/mms-2013-0032>.
- Zoladz M., Kmon P., Rauza J., Grybos P., Blasiak T., 2014, *Multichannel neural recording system based on family ASICs processed in submicron technology*, Microelectronics Journal, vol. 45, no. 9, pp. 1226–1231. <https://doi.org/10.1016/j.mejo.2014.01.018>.